

Study on Electrochemical Behavior of *Horseridash peroxidase* Enzyme by MgO Nanoparticles Modified Electrode to Identify *Hydrogen peroxide*

Hossein Salavati, Mohamad Fazilati, Raheleh Behrooznam*

Department of Biology, Payame Noor University, I.R. of IRAN

*E-mail: r_b1075@yahoo.com

Received: 8 February 2014 / Accepted: 13 October 2014 / Published: 28 October 2014

In this research, the electrochemical behavior of *Horseridash peroxidase* (HRP) enzyme was studied by use of modified carbon paste electrode with Magnesium oxide (MgO) nanoparticles to identify Hydrogen peroxide. Triple electrode system was used in applied electrochemical cell as carbon paste electrode was exploited in forms of bare or modified with MgO nanoparticles as working electrode; saturated calomel electrode (SCE) was used as reference electrode, and platinum electrode was applied as counter electrode. Morphological studies and analyzing the levels of synthesized MgO nanoparticles levels with visible/ultraviolet double beam spectrophotometer, X-ray diffraction and electron microscope. Cyclic voltamograms (CVs) in 10-240 mV distance within phosphate buffer solution 0.1 M (pH=7.0) were studied. Formal potential (E^0) was considered 119 ± 1 mV in contrast with reference electrode (SCE). In designed biosensor, the linear correlation of cathodic peak on different hydrogen peroxide concentrations was measured in 50-400 μ m distance.

Keywords: Horseridash peroxidase (HRP), biosensor, MgO nanoparticles, Hydrogen peroxide

1. INTRODUCTION

Nanotechnology is a term which includes all the state-of-the-art technologies in nano scale field. It could emerge significant evolutions as a premier technology in different sciences [1]. Among these, medical sciences are not excluded and it could foment a revolution in such field. The late technology bears the potential to influence the industrial countries in coming decades [2]. One of applicable nanoparticles in industry and medicine is Magnesium oxide nanoparticle. Magnesium oxide is used in variety of industrial applications as isolation materials and resistant against high temperatures as well as additive element to petroleum [3]. Furthermore, Magnesium oxide is used as a glass composite resistant to heat in liquid crystal display panels, display panels electro-luminance,

plasma display panels, and display florescent tubes [4]. Recently, nanoparticles are became popular in electrochemical and bioelectrochemical processes to facilitate electron transfer stemming from their extra vigilance and efficiency in developed countries and different types of sensors made from nanomaterial are supplied to the market lately [5]. In most studies, designing biosensors by nanomaterial to improve the electrode surface has been largely expanded as a derivation of biotechnology. Nanoparticles play a key role in the industries correlated with electrochemistry such as batteries, electrochemical batteries, sensors, and biosensors design due to their ability to facilitate electron transmission. Whereas, Hydrogen peroxide is a mediator compound in most of enzyme reactions, the precise assessment of which can be significant from the aspects of enzyme reaction control and synthesize [6]. Therefore, production and designing a sensor to assay this compound more accurate, rapid and optimized identification ability from available methods is of great importance [7]. Generally, the advantage of electrochemical biosensor in comparison with other methods is its easy instruction, low burden, homogeneous response and reliability [8]. Presently, determination of Hydrogen peroxide in different types is of great importance; whereas, it is not only a significant analyte in nutritional, pharmaceutical, clinical, industrial and environmental stuffs, but also plays a key role as an enzyme reaction factor in enzyme-associated systems. Different analytic technics have been employed to define Hydrogen peroxide including titration and spectrometry. However, these technics require long analyzing time and costly reagents. As for these problems, electroanalyze method is a more appropriate method because of low identification range and rapid response time, which is able to identify Hydrogen peroxide in cell circle range of living beings [9].

2. MATERIALS AND METHODS

2.1. Reagents

HRP enzyme was obtained from Sigma Corporation. Other stuffs were provided from Mecer Corporation. Utilized electrode for all the experiments was prepared in phosphate buffer solution (PBS) 0.1 M (pH=7) by using Na_2HPO_4 and NaH_2PO_4 0.1 M solution. In development of MgO nanoparticles from Magnesium acetate ($\text{Mg}(\text{CH}_3\text{COO})_2$) 0.14 M, Polyvenil pyrroline ($(\text{C}_6\text{H}_9\text{NO})_n$), Tri-methyl ammonium hydroxide ($(\text{CH}_3)_4\text{NOH}$) and Ethanol ($\text{C}_2\text{H}_6\text{O}$) provided from Mecer corporation were used. All the utilized stuffs were provided by double distilled water.

2.2. Equipment

In utilized electrochemical cell, triple electrode system was used as carbon paste electrode (4mm diameter) in forms of bare or modified with MgO nanoparticles; saturated calomel electrode (SCE) was used as reference electrode as well as a platinum electrode as counter electrode. Notably, the SCEs were provided from Auroumiyeh Azar Electrode Corporation of Iran. Electrochemical studies were carried out on basis of cyclic voltammogram method and by utilizing potentiostat-galvanoacetate device in a way that one side of which was in link with three foregoing electrodes and the other side with a PC for data analyzing and drawing oxidative and reductive charts. Morphological

studies and observation of synthesized MgO nanoparticles levels were accomplished by double beam visible/ultraviolet spectrophotometer TU-1901, Broker X-ray diffraction device with $\text{CuK}\alpha$ radiation, and transmission electron microscope (TEM) JEM-200CX.

2.3. MgO nanoparticles preparation

Initially, 50 mL of Magnesium acetate 0.14 M was sonicated with sufficient proportion of Polyvinyl pyrrolone (PVP) as controlling factor of texture for 30 minutes, afterwards, sufficient extent of Tri-methyl ammonium hydroxide (TMAH) 0.34 M was slowly added to solution. The final achieved residual Magnesium hydroxide was filtered and rinsed with distilled water and Ethanol. 50mL Ethanol was added to the obtained residual and the resulted combination was sonicated for 30 min and filtered subsequently. The final achieved residual was dehydrated for 4 hours in 550°C . MgO nanoparticles were sonicated in Ethanol for 30 min to diminish the bulk form. At the last stage, the compound was filtered and dehydrated in 110°C . The final gained product was powder of MgO nanoparticles to be utilized in later stages of process.

2.4. Preparation of bare carbon paste electrode

Carbon powder (size 50 mm, density 20-30 g/100mL) was blended with binder and silicon oil within a paste made from agate by mortar. Carbon paste electrode was constructed from a proper Teflon tube filled with carbon paste. A copper wire was passed through the prepared paste placed inside the Teflon tube for the carbon paste electrode to connect with the outer circuit electrically. Primarily, the electrode was reconstructed mechanically by some provided paste in upper levels for electrochemical analyses and then glossed by transparent paper.

2.5. Preparation of modified carbon paste electrode with MgO nanoparticles and HRP enzyme

Modified carbon paste electrode with MgO nanoparticles, carbon powder, binder and 10 mg MgO nanoparticles with silicon oil were blended in a paste made from agate to yield the carbon paste which was used to provide modified carbon paste electrode with MgO nanoparticles and HRP enzyme. At this point, the HRP enzyme was immobilized by infusion of 4 μL from 10 mg/mL of protein solution on the surface of carbon paste electrode modified with MgO nanoparticles and dehydrated at room temperature for 45 minutes. The provided electrode was slowly rinsed with double distilled water subsequently.

3. DISCUSSION AND RESULTS

3.1. X-ray diffraction pattern of developed nanoparticles

X-ray diffraction device task is the determination of angles that diffraction process is induced in which according to Bragg relation ($2d\sin\theta=n$). XRD pattern in figure 3-1 is for MgO nanoparticles;

diffraction peaks are absorbed in 2θ value. Maximum peak was used to estimate the pattern size by contribution of Shrer equation [10]. $D = K\lambda / (\beta \cos \theta)$ which K is constant (0.9), λ is wavelength ($\lambda = 1.5418 \text{ \AA}$) (Cu $K\alpha$), β is full width at the half-maximum of line and θ is diffraction angel. The size was achieved by applying density peak for nanoparticles in range of 20-30 nm and the increase in peak sharpness is resulted from crystal-shape nature of nanoparticles which were bound together in order to study diffraction powders.

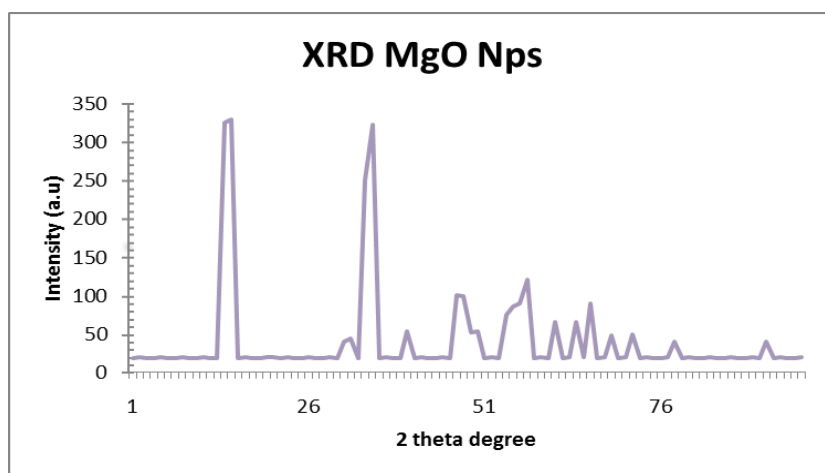


Figure 1. X-ray diffraction model (XRD) of synthetic MgO nanoparticles

3.2. Visible/ultraviolet spectrum properties of MgO nanoparticles

This spectrophotometry is associated with the transferences across electron balances. Such transferences are generally developed between hybrid orbital, or non-hybrid double electrons and anti-hybrid orbital, as a result, wavelength of absorbance peaks can be connected with different hybrids available in under study species.

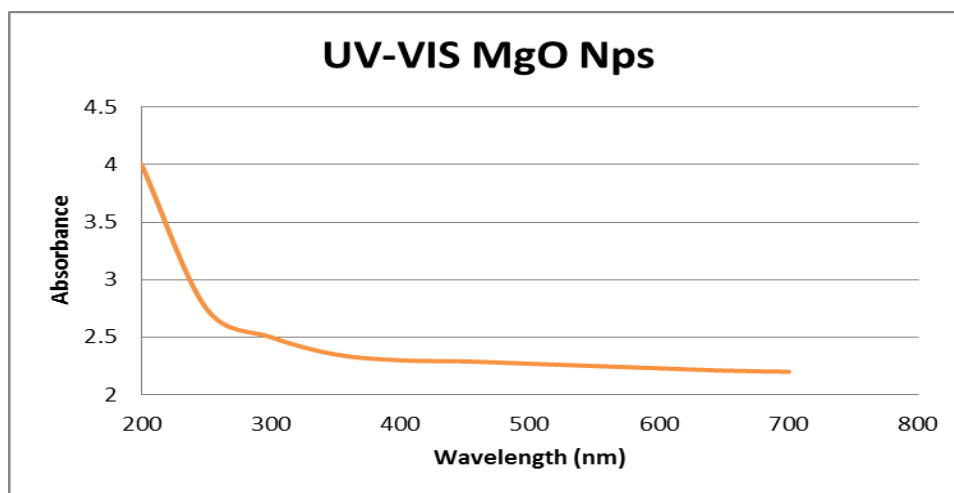


Figure 2. Properties of UV-VIS spectrum of MgO nanoparticles

The most significant specification of nanoparticles is the estimation of optical absorbance spectrum size; inasmuch as UV-VIS absorbance spectrum is an effective technic in visual detection of quantum particles size. UV-VIS spectrum of Magnesium nanoparticles has been shown in figure 3-2. This optical phenomenon suggests the quantum effect of nanoparticle size [11, 12].

3.3. Electron microscope analysis of MgO nanoparticles

The image of Transmission Electron Microscope (TEM) of MgO nanoparticles has been shown in figure 4. Because of the increase in ratio of surface to volume stemming from reduction of smaller size nanoparticles, those are able to play a significant role during immobilization. As for achieved results from TEM analyses, the size of synthesized MgO nanoparticles diameter is within the range of 20-30 nm.

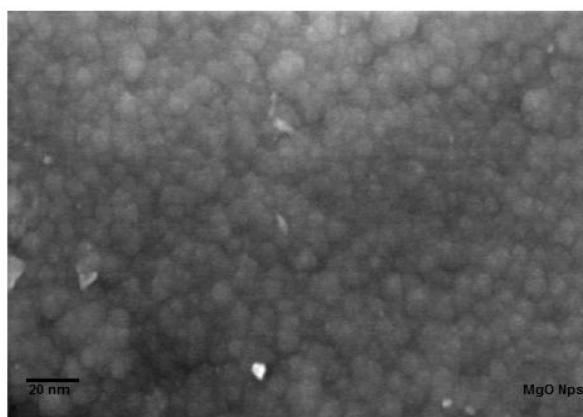


Figure 3. TEM images of synthesized MgO nanoparticles

3.4. Electron direct transference from HRP enzyme on surface of modified carbon paste electrode With MgO nanoparticles

Cyclic voltammometry (CV) was used to study redox alterations in electrodes. Cyclic voltammogram (CVs) of bare carbon electrode and modified carbon paste electrode with HRP enzyme and MgO nanoparticles were studied in distance of 10-240 mV inside phosphate buffer solution 0.1 M (pH=7.0). No redox peak was observed in bare electrode in absence of MgO nanoparticles and Horseridash peroxidase enzyme (figure 3-4 a). In comparison with former electrode, two explicit and reversible oxidative and reductive peaks in modified electrode with MgO nanoparticles were observed, which suggests that the area of effective surface of electrode has significantly increases due to utilization of MgO nanoparticles. Although cyclic voltammometry of modified carbon paste electrode with HRP enzyme and MgO nanoparticles were represented a double oxidative and revival peaks in 130 and 107 at the rate of about 100 mV/s respectively (figure 3-4 b), specifications of double redox peaks $\text{Fe}^{(\text{III})}/\text{Fe}^{(\text{II})}$ HRP enzyme, suggests that electron direct transfer between HRP enzyme and modified electrode with MgO nanoparticles is established. Difference between potential rates of

cathodic and anodic peaks is calculated as $\Delta E = 27$ Mv. Redox peaks represent that the location of HRP enzyme redox reaction is electroactive center. Formal potential (E^0) had been 119 ± 1 – mV for redox reaction of HRP enzyme on modified carbon paste electrode by HRP enzyme and MgO nanoparticles exposing reference electrode (SCE). Formal potential (E^0) in all electrochemical studies has been estimated as the center point of oxidation and revival. MgO nanoparticles can facilitate direct electron transfer between proteins and electrode surface. It is reported that proteins with prosthetic additionally, can catalyze the reactions associated with Hydrogen peroxidase as catalyzer; HRP enzyme is one of these enzymes which has been used in this project. This protein-based structure is able to convert oxidative Iron form (Fe^{3+}) to revival form (Fe^{2+}) by electron transference [13].

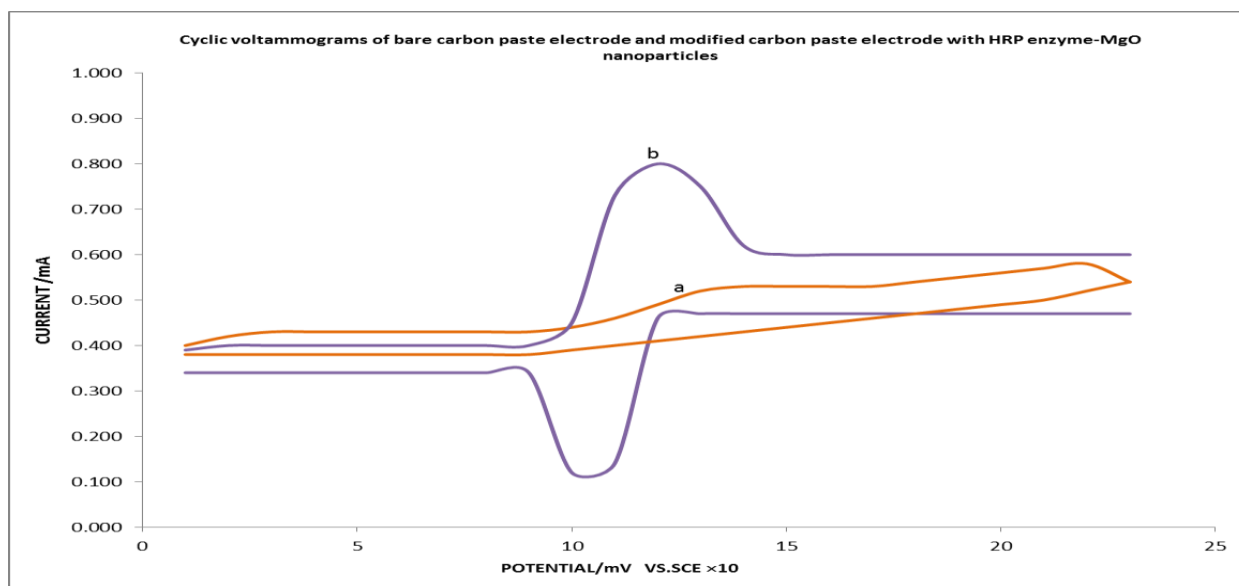


Figure 4. cyclic voltammogram, (a) bare carbon paste electrode and (b), modified carbon paste electrode with MgO nanoparticles and HRP enzyme; scan rate 100 mV/s and in phosphate buffer solution 0.1 M and pH=7.

Figure 3-5 (a): cyclic voltammograms for modified electrode with HRP enzyme and MgO nanoparticles in phosphate buffer solution 0.1 M (pH=7.0) show different rates from 100mVs^{-1} to 600mVs^{-1} . In a homogeneous rate, cathodic and anodic peaks increase along with rate linearly. As shown in figure 3-5 (b), redox peaks increase along with the increase in scan rate linearly, correlation ratio is 0.9974 ($i_{pc} = -0.0033v + 0.4067$), and for cathodic and anodic peaks is 0.9981 ($i_{pa} = 0.005v + 0.1933$). These calculated values confirm the correct stable immobilization of HRP enzyme on surface of carbon paste electrode as well as the effective role of MgO nanoparticles as facilitators of electron direct transference. Results of studies are applicable to define the rates of HRP enzyme in phosphate buffer solution.

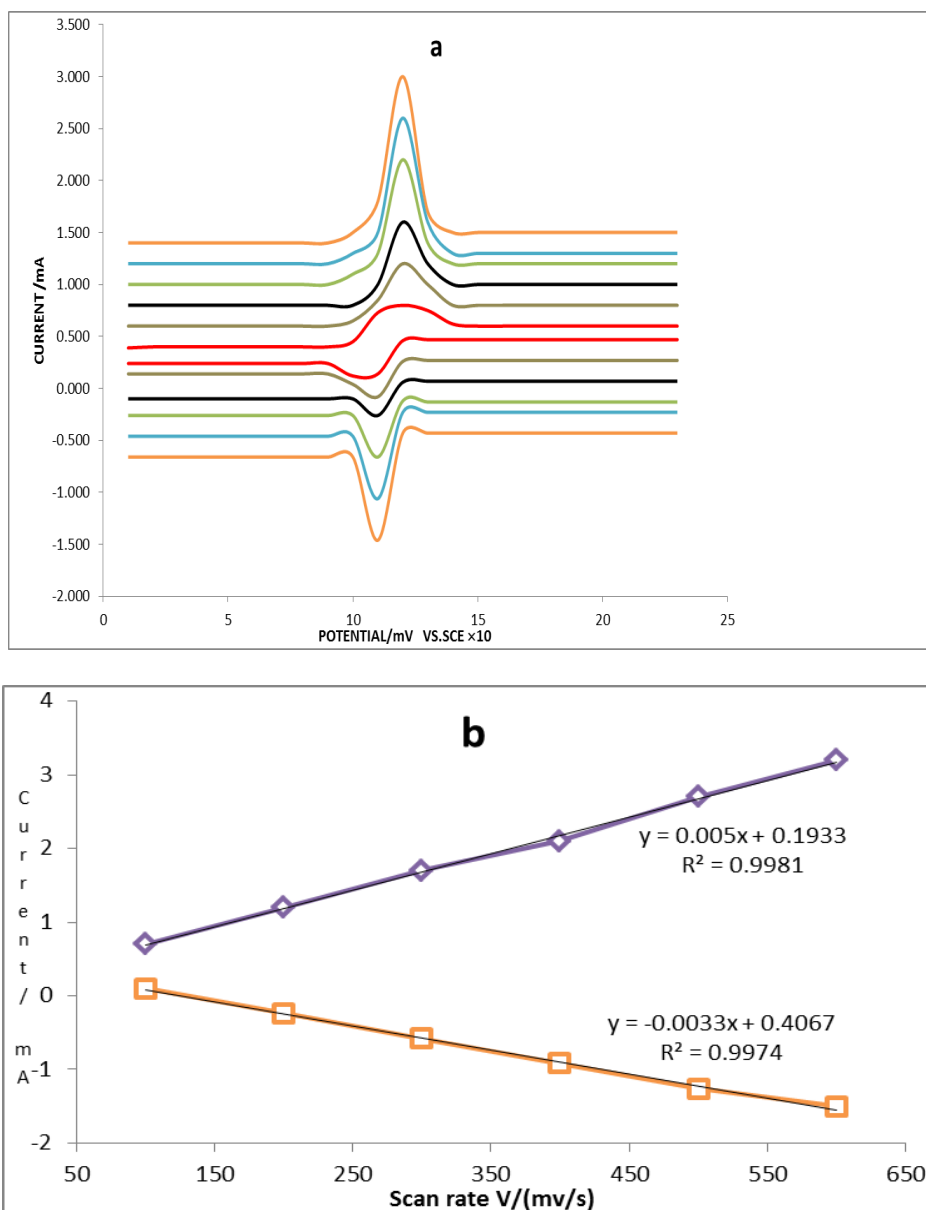


Figure 5. (a) cyclic voltammograms of modified carbon paste electrode by HRP enzyme and MgO nanoparticles in different rates, from inside to outside; 100, 200, 300, 400, 500, and 600 mV/s and (b), relation between cathodic and anodic peaks (ipa, ipc) vs, purple lines are anodic peaks and orange lines are cathodic peaks.

All these results suggest that HRP enzyme is mobilized on controlled surface of modified electrode with MgO nanoparticles. The presence of Fe (II/III) in HRP enzyme is a significant factor that allows it to appear in electrochemical reactions particularly oxidation and reduction reactions; all these reactions are along with electron transfer where Fe (III) is oxidative status and Fe (II) is reductive status. When peak-to-peak separation or energy difference (ΔE) is larger than 200 mV, electron transfer rate constant (k_s) is achieved readily by Laviron relations noted here [14,15,16]:

$$E_{p,cathodic} = E^0 + \frac{RT}{\alpha F} \ln \frac{RTk_s}{\alpha Fv} \quad (1)$$

$$E_{p,\text{anodic}} = E^0 + \frac{RT}{(1-\alpha)F} \ln \frac{RTk_s}{(1-\alpha)Fv} \quad (2)$$

$$\Delta E_p = E_{p,\text{anodic}} - E_{p,\text{cathodic}} = \frac{RT}{\alpha(1-\alpha)F} \quad (3)$$

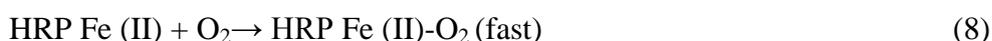
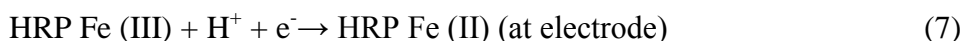
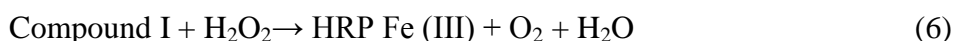
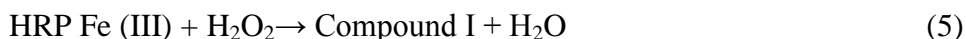
$$\left[\log k_s = \alpha \log (1-\alpha) + (1-\alpha) \log \alpha - \log \frac{RT}{nFv} - \frac{\alpha(1-\alpha)nF\Delta E_p}{2.3 RT} \right] \quad (4)$$

Where, α is electron transfer coefficient and n is number of transferred electrons. R , T , and F are coefficients of gases, absolute temperature and Faraday coefficient respectively, that these three parameters values are defined.

($R = 8.314 \text{ J mol}^{-1} \text{ K}^{-1}$, $F = 96493 \text{ C/mol}$, $T = 298 \text{ K}$). Transfer rate constant can be achieved from ΔE_p equate $\ln v$. In this research, calculated value for electron transfer rate constant (k_s) was considered equal to 1.9 s^{-1} and α value equal to 0.55. High level of computed digital value for electron transfer rate constant (k_s) directly represents that modified carbon paste electrode with NiO nanoparticles and catalase enzyme has more increasing rate to transfer electron between catalase enzyme and carbon paste electrode.

3.5. Hydrogen peroxide biosensor design by using revival peaks of modified carbon paste Electrode with HRP enzyme

Electrocatalytic reaction of modified electrode with HRP enzyme and MgO nanoparticles exposing Hydrogen peroxide was studied by cyclic voltammogram in this section. In image 6, different cyclic voltammograms for Hydrogen peroxide biosensor within phosphate buffer 0.1 M (pH=7.0) are shown that are included of Hydrogen peroxide different concentrations in the absence of oxygen. Catalytic revival of Hydrogen peroxide in designed biosensor by means of modified electrode with HRP enzyme and MgO nanoparticles has been explicitly shown in figure 6(a). By addition of Hydrogen peroxide, revival peak is sequentially increased; whereas, oxidation peak is decreased (figure 6a) which is resulted from electrocatalytic revival procedure of Hydrogen peroxide. It can be concluded from this study that, HRP enzyme is immobilized on MgO nanoparticles and shows the proper catalytic activity relating to Hydrogen peroxide. Reduction of oxidative peak was accompanied with elevation of HRP enzyme and MgO nanoparticles revival peaks. Electrocatalytic process can be expressed as follows:



Calibration diagram of figure 6(b) represents a linear correlation of cathodic peak on different concentrations of Hydrogen peroxide in 50-400 μm distances. In figure 6(b), at higher Hydrogen peroxide concentration than shown range, the height of cathodic peak decreases and remains constant.

As seen, response of designed biosensor on basis of modified electrode with HRP enzyme and MgO nanoparticles represents the proper linear relation in this distance; the correlation ratio has been achieved as $0.9916 R^2$.

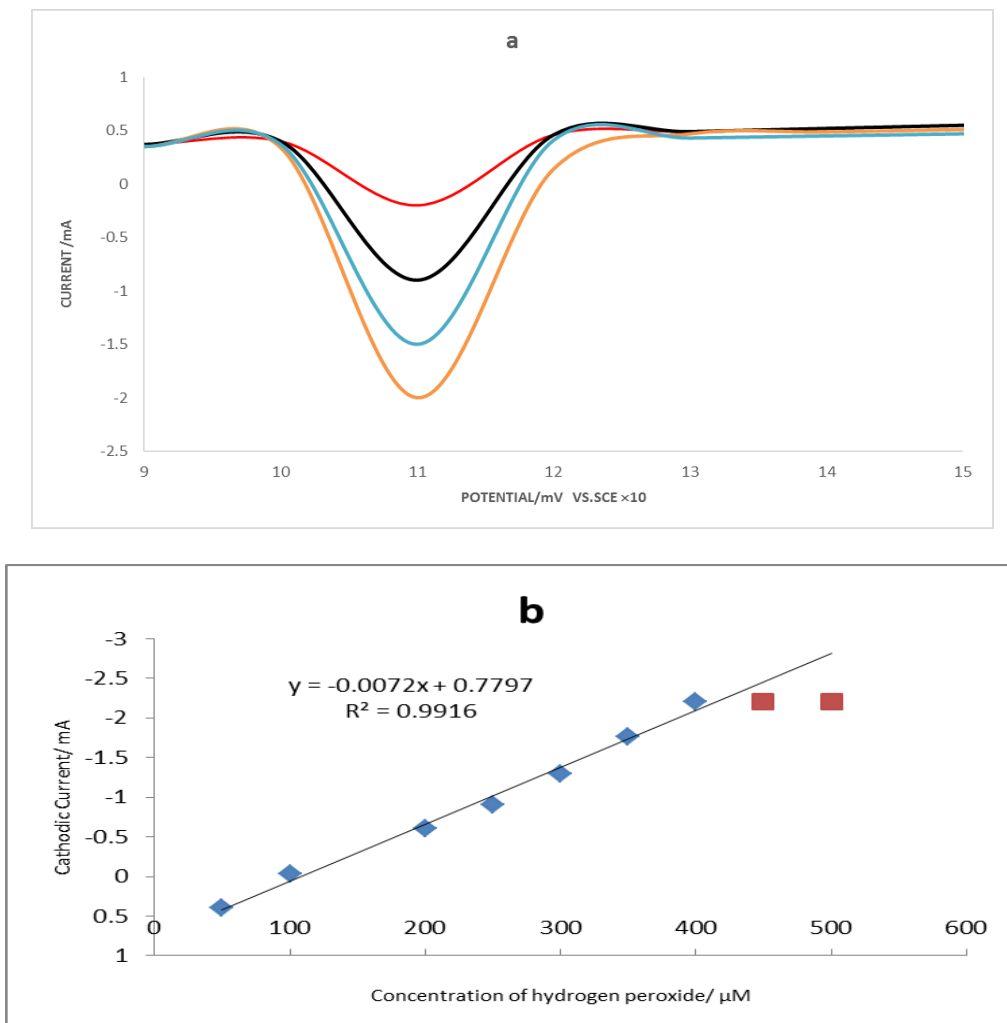


Figure 6. (a): cyclic voltammograms for modified electrode with HRP enzyme and MgO nanoparticles in phosphate buffer solution 0.1 M (pH=7.0) for different Hydrogen peroxide concentrations and (b) connection between cathodic peak of HRP enzyme and different concentrations of hydrogen peroxide (rate: 100 mVs^{-1}).

3.6. Effect of pH on biosensor response

In order to develop proper biosensor for Hydrogen peroxide, this biosensor was exposed to different pHs. The effect of pH under constant concentration of Hydrogen peroxide ($50 \mu\text{M}$) for modified electrode with HRP enzyme and MgO nanoparticles has been shown in figure 7. As it is shown, the maximum response was obtained at pH 7.0. Therefore, applying PBS with pH 7.0 was an appropriate choice. pH 7.0 was the best biosensor response in this section [17].

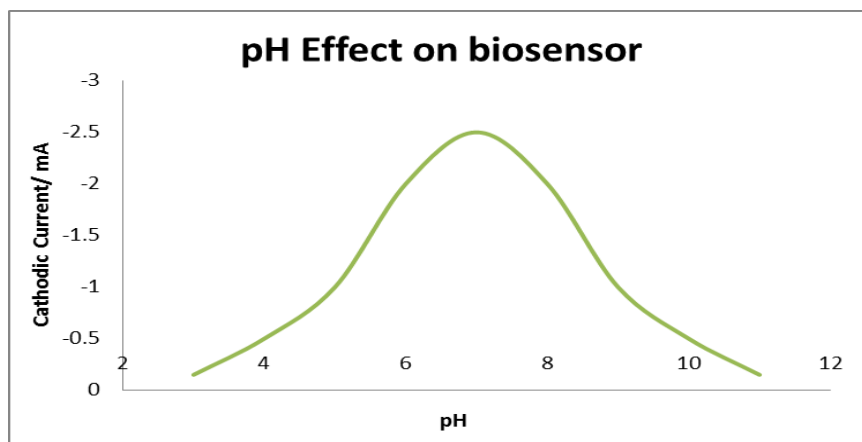


Figure 7. Diagram of biosensor response to pH modifications; maximum observed response is at pH 7.0.

3.7. Stability of designed biosensor in definition of Hydrogen peroxide

Designed biosensor was analyzed from the aspect of stability. Inasmuch as in this research enzymic texture was used, one of the most important factors in protection of biosensor stability had been inhibition of denaturation associated with enzyme texture. Primary activity and biosensor response rate were measured for 21 hours and up to reach to a constant value. To test stability, designed biosensor was kept in refrigerator at 3°C as well as the temperature of 40°C; the biosensor reserved 85% and 77% of its primary activity respectively. Furthermore, it was disclosed that designed biosensor has a high reproducibility; it was found that, the interface factors such as Ascorbic acid have no explicit role in biosensor activity reduction [18, 19]. In research by Koorosh Fooladsaz1 a biosensor designed based on catalase (CAT) and modified carbon paste electrode (CPE) with zinc oxide (ZnO) nanoparticles for Determination level of dopamine by electrochemical methods. The CAT / ZnO Nps/ CPE showed a good sensitive state towards oxidation of DA. The designed biosensor showed a good stability and retains its 91% activity after 21 days [20]. In research, direct electron transfer of cytochrome c (cyt. c)--a model for studying the electron transfer of enzymes is achieved at hexagonal ZnO nanosheets by one-step electrodeposition. Experiment data show, under the optimized potential of 0.0 V (vs. AgAgCl), the electrochemical determination of H₂O₂ is free from not only anodic interferences like ascorbic acid (AA) and dopamine (DA), but also a cathodic interference-O₂ [21].

4. CONCLUSION

Designing biosensor by benefiting from nanotechnology was noticed by many researchers in recent years. In the present study, MgO nanoparticles were used as electron conveyors between HRP enzyme and modified electrode with Magnesium oxide. Results of study lead to design novel biosensor in order to detect Hydrogen peroxide. This study presented that the biosensor has rapid response, high sensitivity, reproducibility, and high stability.

References

1. G. Bystrzejewska-Piotrowska, J. Golimowski, and P.L. Urban, *Waste Management*, 29(2009) 2587.
2. J. Kuzma, and J. Besley, *NanoEthics*. 2(2008) 149.
3. W. Yang, J.I. Peters, and R.O. Williams III. *International Journal of Pharmaceutics*. 356(2008) 239.
4. L. Aghebati-maleki, B. Salehi, R. Behfar, H. Saeidmanesh, F. Ahmadian, M. Sarebanhassanabadi, M. Negahdary. *Int. J. Electrochem. Sci.* 8(2013): 257.
5. A.J. Haes, and R.P. Van Duyne. *Laser Focus World*. 39(2003):153.
6. A.J. Haes, R.P. Van Duyne. *Mat Res Soc Symp Proc*. 2002; 23(2007):1.
7. H.A. Clark, M. Hoyer, M.A. Philbert, R. Kopelman. *Anal Chem*. 71(1999) 4831.
8. T. Vo-Dinh, G.D. Griffin, J.P. Alarie, B. Cullum, B. Sumpter, and D.J. Noid. *Nanopart. Res.* 2(2000) 17.
9. C. Jianrong, M. Yuqing, H. Nongyue, Wu. Xiaohua, Li. Sijiao. *Biotechnology Advances*. 22 (2004)505.
10. L. Monico, G. Snickt, Koen Janssens, W. Nolf, C. Miliani, J. Dik, M. Radepont, E. Hendriks, M. Geldof, and M. Cotte. *Anal. Chem.* 83 (2011), 1224.
11. L. Sooväli, E.-I. Rõõm, A. Kütt, I. Kaljurand, I. Leito. *Accred. Qual. Assur.* 11(2006) 246-255.
12. Skoog, Principles of Instrumental Analysis. 6th ed. *Thomson Brooks/Cole*, (2007) 349.
13. R. Malekzadeh, M. Negahdary, A. Farasat, M. Torkamani Noughabi, et al. *European Journal of Experimental Biology*, 2 (2012):454.
14. E. Laviron. *Journal of Electroanalytical Chemistry*, 101(1979) 19.
15. E. Laviron. *Journal of Electroanalytical Chemistry*. 100(1979) 263.
16. Y. Wu, Q. Shen, S. Hu. *Anal. Chim. Acta* 558(2006) 179.
17. A.M. Bond. *Modern Polarographic Methods in Analytical Chemistry*, Marcel Dekker, New York. 1980.
18. C. Matsubara, N. Kawamoto, K. Takamura. *Analyst* 117 (1992) 1781.
19. L. Luo L, Z. Zhang. *Anal Chim Acta* 580(2006) 14.
20. K. Fooladsaz, M. Negahdary, G. Rahimi, A. Tamijani, S. Parsania, H. Akbari-dastjerdi, A. Sayad, A. Jamaledini, F. Salahi and A. Asadi. *Int. J. Electrochem. Sci.*, 7 (2012) 9892.
21. Q. Rui, K. Komori, Y. Tian, H. Liu, Y. Luo, Y. Sakai. *Anal Chim Acta*. 670(2010):57.

© 2014 The Authors. Published by ESG (www.electrochemsci.org). This article is an open access article distributed under the terms and conditions of the Creative Commons Attribution license (<http://creativecommons.org/licenses/by/4.0/>).